Pharmaceutical Research, Vol. 24, No. 9, September 2007 (© 2007)
DOI: 10.1007/s11095-007-9277-5

Research Paper

Enhanced Intercellular Retention Activity of Novel pH-sensitive Polymeric Micelles in Wild and Multidrug Resistant MCF-7 Cells

Ghazal Mohajer,[1] Eun Seong Lee,[1] and You Han Bae[1]

Received November 21, 2006; accepted February 20, 2007; published online March 24, 2007

Purpose. The purpose of this work was to demonstrate the advantage of using pH-sensitive polymeric mixed micelles (PHSM) composed of poly(L-histidine) (polyHis)/poly(ethylene glycol) (PEG) and poly(L-lactic acid) (pLLA)/PEG block copolymers with folate conjugation to increase drug retention in wild-type and MDR tumor cells.
Materials and Methods. Both wild-type and multidrug resistant (MDR) human breast adenocarcinoma (MCF-7) cell lines were used to investigate the accumulation and elimination of doxorubicin (DOX), PHSM with folate (PHSM/f), and pH-insensitive micelles composed of pLLA/PEG block copolymer with folate (PHIM/f).
Results. Cells treated with PHSM/f showed decelerated elimination kinetics compared to cells treated with PHIM/f. MDR cells treated with drug-containing PHSM/f for 30 min retained 80% of doxorubicin (DOX) even after incubation for 24 h in the absence of drug. On the other hand, cells treated with drug-containing PHIM/f retained only 40% of DOX within the same period of time. Flow cytometry and confocal microscopy confirmed these results.
Conclusions. Cellular entry of the micelles occurred via receptor-mediated endocytosis using folate receptors. The pH-induced destabilization of PHSM/f led to rapid distribution of drug and polymer throughout the cells, most likely due to polyHis-mediated endosomal disruption. This reduced the likelihood of drug efflux via exocytosis from resistant tumor cells.

KEY WORDS: exocytosis; folate; multidrug resistance; pH-sensitive polymeric micelle; poly(L-histidine).

INTRODUCTION

Treatment of tumors with chemotherapeutic agents is often complicated by the phenomenon of multidrug resistance (MDR). MDR is the resistance of tumor cells to several anti-tumor drugs of unrelated structural classes and mechanisms of action (1), due to increased efflux activity. In addition to P-glycoprotein (Pgp) on the plasma membrane of MDR tumor cells, an increasing number of ATP-driven efflux pump families have been identified that confer MDR, the most well-known being the multidrug resistance proteins MRP1, MRP2, MRP3, etc., which are all highly over-expressed in MDR tumor cells (2–5).

One efflux mechanism in MDR tumor cells is characterized by increased exocytosis of anti-tumor drugs via endosomal vesicle recycling (6–9). It seems that the intracellular pH shift in the MDR tumor cells affects the rates of vesicular transport and exocytosis (10, 11). The presence of the MDR-related protein, Pgp, may lead to increased exocytosis (12). The MRP family of proteins, found predominantly on intracellular organelles, is expected to play a significant role in the exocytosis process (7, 12–16). However, the exact mechanism of exocytosis of anti-tumor drugs in MDR tumor cells is still unclear, and the exocytosis of drug-encapsulated nano-carriers in MDR tumor cells is relatively unknown.

A few studies have been published that investigated the exocytosis of nano-carriers in wild-type tumor cells. Panyam and Labhasetwar (17) reported that nanoparticles were rapidly taken up within 1 min of incubation but 65% of the internalized fraction was exocytosed in 30 min. Cells in serum-free medium showed inhibition of nanoparticle exocytosis, suggesting that proteins in the medium probably interact with the vesicle-recycling pathway and induce increased exocytosis of nanoparticles. Park et al. (18) found that active exocytosis of nanoparticles in HeLa cells depended on the pre-incubation time. The quantity of nanoparticles that were removed through exocytosis decreased with increased pre-incubation time. Sahoo and Labhasetwar (19) investigated cellular efflux behavior of paclitaxel-loaded nanoparticles with the specific ligand, transferrin. They reported that transferrin-conjugated nanoparticles showed relatively reduced exocytosis compared to transferrin-unconjugated nanoparticles. However, this result may not be consistent with other various ligand/receptor mediated endocytosed nanoparticles. In one study, the accumulation of folate-PEG-liposomal DOX by KB cells

[1] Department of Pharmaceutics and Pharmaceutical Chemistry, University of Utah, 421 Wakara Way, Suite 315, Salt Lake City, UT 84108, USA.
[2] To whom correspondence should be addressed. (e-mail: you.bae@utah.edu)

was 45-fold higher than for non-targeted liposomal DOX (20, 21). Nevertheless, the MDR families may mediate transport of folate-conjugate from intracellular organelles such as endosomes to the extracellular space (9, 13, 14, 22).

In order to maximize ligand/receptor mediated drug carrier delivery and drug accumulation in tumor cells, the kinetics of drug delivery must exceed the efflux kinetics. One approach towards increasing drug accumulation is suppressing the efflux mechanism.

The probable endosomal disruption or fusogenic activity of polyHis has recently served as a tool in advancing systems for non-viral gene delivery (23–25). Previous experimentation showed that polyHis caused membrane disruption of endosomes and lysosomes. Endosomal membrane destabilization occurs due to the proton-sponge effect of polyHis that is caused by the protonation of its imidazole groups, which in turn interact with negatively-charged membrane phospholipids (26–30). This interaction facilitates the entry of DNA/polymer complexes into the cytoplasm of the cell, thereby increasing gene transfection efficacy.

Our group recently prepared and used polyHis/PEG to construct polymeric micelles that responded to slight acidity (pH 7.0–6.4) and resulted in micelle destabilization (26–29, 31, 32). This accelerated drug release and widespread cellular distribution of DOX. In this study, we demonstrate the advantage of using PHSM/f to increase drug retention in MDR tumor cells. Folate was selected as the specific ligand for effective internalization of micelles into tumor cells. Overexpression of the folate receptor in a large number of cancers has led to the use of folate-mediated tumor cell targeting of anti-tumor drugs (20, 21, 26, 27).

MATERIALS AND METHODS

Materials

L-glutamine, *n*-propyl galate, glycerol, bovine serum albumin (BSA), HEPES, DOX·HCl, and CellLytic™M Cell Lysis Reagent were purchased from Sigma Chemical Company Inc. (St. Louis, USA). Formaldehyde, fluorescence isothiocyanate (FITC), HCl, NaOH, and $Na_2B_4O_7$ were purchased from Aldrich Chemical Company, Inc. (Milwaukee, USA). Dimethylsulfoxide (DMSO) was purchased from J. T. Baker (Deventer, Netherlands). Penicillin-streptomycin, Tris–HCl (pH 8.4), fetal bovine serum (FBS), 0.25% (w/v) Trypsin-0.03% (w/v) EDTA solution, Dulbecco's phosphate-buffered saline, phosphate buffered saline (PBS, pH 7.4), and RPMI1640 medium were purchased from Gibco Co. (Uxbridge, U.K). PolyHis/PEG and pLLA/PEG block copolymers were synthesized as previously reported (26–29, 31, 32). The molecular weight of synthesized polyHis/PEG was 7 kDa, composed of 5 kDa polyHis block and 2 kDa PEG block; molecular weight for pLLA/PEG was 5 kDa (pLLA 3 kDa and PEG 2 kDa).

Methods

Preparation of FITC-labeled Polymeric Micelles

All polymer molecules used in this study were conjugated to folate. The FITC-labeled, PHSM/f and PHIM/f were prepared using polyHis/PEG with folate (polyHis/PEG-folate) and FITC-pLLA/PEG with folate (FITC-pLLA/PEG-folate) (26–28). The weight ratio of polyHis/PEG-folate to FITC-pLLA/PEG-folate for the micelles was 60/40 for PHSM/f and 0/100 for PHIM/f. Preparation of the FITC-labeled micelles was achieved by dissolving the appropriate weight ratios of polymer constituents in DMSO solvent; subsequent steps identical to the preparation of DOX-loaded micelles.

Preparation of DOX-loaded Polymeric Micelles

DOX-loaded PHSM/f (average particle size=73 nm by dynamic light scattering) or PHIM/f (average particle size=82 nm by dynamic light scattering) were prepared as previously reported (26, 27). DOX was loaded by dissolving DOX (10 mg) and the appropriate weight ratio of the polymeric constituents (50 mg) in DMSO. This solution was transferred to a preswollen dialysis membrane (Spectra/Por molecular weight cut-off 15,000). The product was dialyzed against HCl-$Na_2B_4O_7$ buffer solution (pH 9.0) for 24 h at 4°C and the medium was exchanged several times. The product was subsequently lyophilized until further use. The amount of DOX loaded was determined by measuring the UV absorbance of the drug-loaded polymeric micelles in DMSO at 481 nm. In preliminary release studies with DOX-loaded micelles, there was no noticeable burst effect and less than 40% of loaded drug was released after exposure to pH 6.8 buffer media for 24 h. The drug release pattern followed first order kinetics. As the pH dropped from pH 6.8 to pH 6.0 (endosomal pH) the amount of DOX released from the micelles rose to 80% in 24 h. These results were consistent with our previous reports (26–29, 31, 32).

Accumulation of FITC-labeled Polymer

The human breast adenocarcinoma (MCF-7) cell line (from ATCC) was used in the following experiments. DOX-resistant MCF-7 cells (MCF-7/DOX^R) were created by selecting live MCF-7 cells following stepwise exposure to free DOX at 0.001–10 μg/ml (26). Wild-type and DOX-resistant cells were maintained in RPMI-1640 medium with 2 mM L-glutamine, 5% penicillin-streptomycin and 10% FBS in a humidified incubator at 37°C and 5% CO_2 atmosphere.

To test FITC-labeled PHSM/f or PHIM/f against wild MCF-7 or MCF-7/DOX^R cells, confluent cells were harvested and seeded at 5×10^4 cells/ml in a 96-well plate in 100 μl of RPMI-1640 medium for at least 24 h prior to experimentation to allow cells to adhere to the plate surface. FITC-labeled PHSM/f or PHIM/f in RPMI-1640 medium (in PBS at pH 7.4, 6.8 or 6.2) were prepared immediately before use. The micelle solutions (polymer concentration=5 μg/ml) were added to the cell samples and incubated at 37°C for 0.5, 2, 4, 6, 8, 18, and 24 h. The cellular accumulation of the micelles was assessed by fluorometry. After removing the medium, cells were lysed using CellLytic™M Cell Lysis Reagent (125 μL), and the fluorescein content was measured by assaying the cell lysate using static fluorescence measurements (excitation and emission wavelengths of 488 and 520 nm, respectively). The accumulation of polymeric micelles was assessed as the mean

fluorescence ratio (MFR) using the formula MFR(%)=[(f_s/f_c)/f_t]×100, where f_s is the mean fluorescence of treated cells, f_c is the mean fluorescence of control cells (untreated), and f_t is the mean fluorescence of total FITC-labeled polymer.

Confocal Microscopy

The intracellular distribution of FITC-labeled polymers in PHSM/f or PHIM/f was carried out using MCF-7/DOX^R cells (26) grown on a Lab-Tek^R II chamber slide (Nalge Nunc International, Napevillem, IL). Cells maintained at pH 6.8 (this pH was used throughout these experiments to mimic the acidic tumor environment) were incubated with each polymeric micelle type for 30 min (and potentially incubated for 1 to 2 h in fresh medium with no micelles), washed three times with PBS pH 6.8 and then fixed with 1% formaldehyde in PBS for 10 min. A coverslip was mounted on a glass microscope slide with a drop of anti-fade mounting medium (5% *N*-propyl galate, 47.5% glycerol and 47.5% Tris–HCl at pH 8.4). The specimens for fluorescein detection were examined under a confocal microscope (Leica TCS NT, Leica, Germany) with excitation and emission wavelengths of 488 and 510 nm, respectively.

Flow Cytometry Analysis

MCF-7/DOX^R cells (1×10^6 cells/ml) were harvested, pelleted by centrifugation (1,000 rpm for 3 min) and resuspended in RPMI-1640 solution at pH 6.8. Cells were incubated at pH 6.8 for 30 min in RPMI-1640 solution containing FITC-labeled polymeric micelles (polymer concentration=5 μg/ml). Unbound micelles were removed by gentle pipetting, and cells were rinsed with PBS pH 6.8 supplemented with 0.5% BSA and 20 mM HEPES. Cells were then incubated for 0.5, 1 or 2 h with fresh RPMI-1640 solution (without polymeric micelles). Cells were collected, pelleted by centrifugation, resuspended in 1 ml of PBS solution supplemented with 0.5% BSA, and analyzed using a flow cytometer (Becton Dickenson FacScan).

Pulse-chase Experiments with DOX and FITC-labeled Polymer

Cells were prepared and seeded as described in Section 2.6. DOX-loaded polymeric micelles (PHSM/f or PHIM/f) and free DOX (DOX concentration=0.5 μg/ml) were added to the cells and incubated at 37°C for 30 min. Initial DOX levels in wild tumor cells were 0.36±0.03 μg/ml (PHSM/f), 0.34±0.02 μg/ml (PHIM/f), and 0.22±0.04 μg/ml (free DOX). Initial DOX levels in MCF-7/DOX^R cells were 0.35±0.02 μg/ml (PHSM/f), 0.33±0.03 μg/ml (PHIM/f), and 0.04±0.02 μg/ml (free DOX).

To study elimination kinetics, buffer containing any residual DOX-loaded polymeric micelles or free DOX was replaced with fresh buffer. Cells were exposed to the fresh buffer for 0.5, 2, 4, 6, 8, 18, and 24 h. The fresh buffer was promptly removed and the remaining (treated) cells were lysed. The cell lysate was analyzed by fluorescence measurements as described above.

The elimination of the FITC-conjugates in the cells was measured in the same manner that DOX accumulation was measured as described above. Initial polymer concentrations in the cells after treatment for 30 min were 2.6±0.3 μg/ml (PHSM/f), 2.4±0.3 μg/ml (PHIM/f) in wild tumor cells, and 2.5±0.2 μg/ml (PHSM/f), 2.3±0.4 μg/ml (PHIM/f) in MCF-7/DOX^R cells. The excitation and emission wavelengths used were the same as for FITC.

Statistical Analysis

All results were analyzed by student *t*-test or ANOVA test with $p<0.05$ significance.

RESULTS AND DISCUSSION

Our group recently reported the creation and use of novel pH-sensitive polymeric mixed micelles composed of polyHis/PEG and pLLA/PEG block copolymers with or without folate conjugation (26, 27). Micelles were investigated for folate receptor-mediated internalization and pH-dependent drug release of loaded DOX. Micelles showed accelerated DOX release with decreasing pH. Further studies compared PHSM/f with PHIM/f using confocal microscopy. There was significant localization of DOX in the endosomal compartments for PHIM/f, compared to broad cytosolic distribution for PHSM/f (26–28). This difference is attributed to endosomal disruption following the destabilization of PHSM/f. This observation prompted a study to compare the delivery of DOX using PHSM/f and PHIM/f in MDR tumor cells. As shown in Fig. 1, we hypothesized that PHSM/f may induce broad cytosolic distribution of drug or polymer following endosomal disruption and triggered drug release, thereby reducing exocytosis of micelles.

Cellular Retention of Micelles

The accumulation kinetics of FITC-labeled, PHSM/f and PHIM/f were similar for both wild-type MCF-7 and MCF-7/DOX^R cells at pH 6.8. As shown in Fig. 2, the differences in the uptake of the two micelle types in either resistant (Fig. 2a) or wild-type (Fig. 2b) tumor cells was negligible. This suggests that both PHSM/f and PHIM/f employ the same method of entry into the cells, which in this case should be folate-mediated endocytosis (21). Since both tumor cell types contain a similarly high number of folate receptors, neither presented a significant advantage for entry (or uptake) over the other (20, 21).

Further investigations showed that decreasing the applied pH resulted in slightly decreased accumulation of DOX (data not shown), similar to relationships already reported in the literature (33). However, these effects were not significant.

The intracellular distribution of PHSM/f or PHIM/f in MCF-7/DOX^R cells was determined through confocal microscopy. As shown in Fig. 3, the confocal images demonstrate that pH-induced micelle destabilization (26–29,

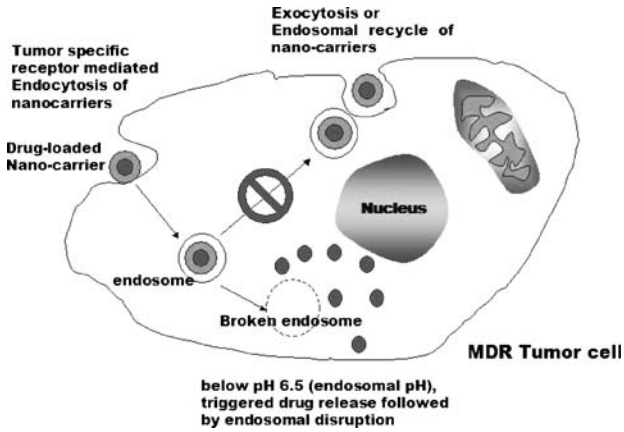

Fig. 1. The proposed design concept of PHSM/f for effective anti-tumor drug delivery to MDR tumor cells. Carriers are constructed so that cellular entry is through receptor-mediated endocytosis, and the polymeric components allow changes in release rate through a pH-activated switching mechanism and also contain fusogenic activity.

31, 32) led to widespread distribution of DOX in the cytosol of tumor cells, as opposed to sequestration of PHIM/f counterparts in intracellular compartments (such as lysosomes). These results are consistent with several other studies where the combined effects of pH-sensitivity and endosomal disruption ability of a polymeric system (34–36) have been applied to tumor cell recognition and gene therapy studies.

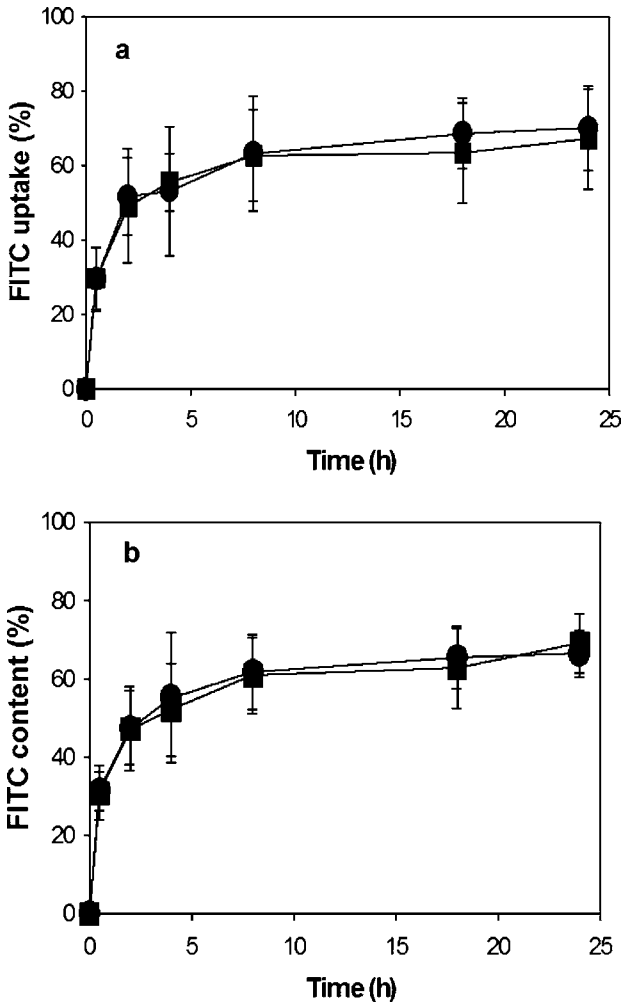

Fig. 2. The percentage of fluorescein content from accumulation experiments measured in samples exposed to FITC-labeled PHSM/f (*filled circle*) or PHIM/f (*filled square*) ($p>0.1$ compared to FITC-labeled PHSM/f) as a function of time against **a** MCF-7/DOX^R cells and **b** wild MCF-7 cells ($n=7$).

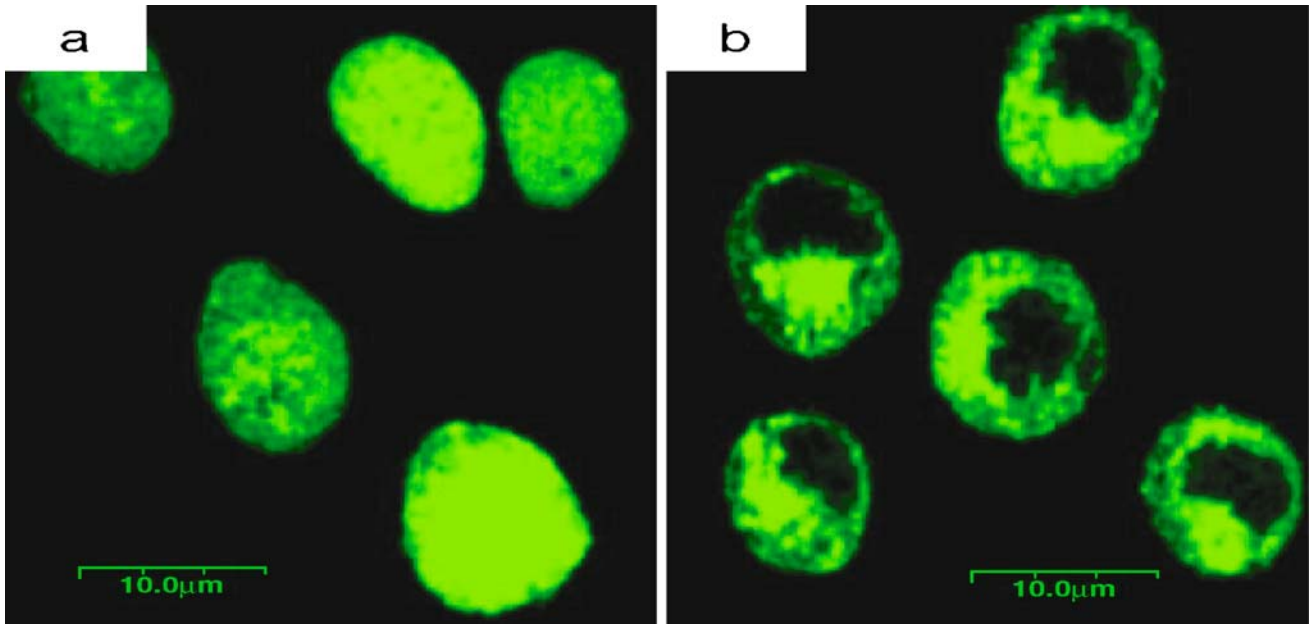

Fig. 3. Confocal microscopic pictures revealing MCF-7/DOX^R cells marked with FITC-labeled polymer after cellular exposure to PHSM/f (**a**) or PHIM/f (**b**) for 30 min and washing.

The elimination of FITC-labeled polymer from MCF-7/DOX^R cells over time is shown in Fig. 4. By measuring the fluorescence intensity in a sample at three time points, the amount of FITC-labeled polymer remaining over time was quantified by flow cytometry.

Fig. 4a shows the exposure of three resistant cell samples to PHSM/f. The relative intensities showed decreased fluorescence with increased incubation time. Fig. 4b shows the exposure of three resistant cell samples to PHIM/f. It is evident that the relative intensity peaks of the PHIM/f samples vary more in relation to one another than for the PHSM/f. While the intensity peak for PHIM/f at 30 min is similar to the intensity peak for PHSM/f at 30 min, at the 1 h time point it becomes evident that the fluorescence intensity for PHIM/f has sharply decreased, and dropped even further after 2 h. This decrease is due to high elimination (exocytosis) rates which are characteristic of cells exposed to PHIM/f. Fig. 4c shows the fluorescence of the control.

Flow cytometry analysis confirmed that PHIM/f demonstrated more rapid efflux than their PHSM/f counterparts. Thus, PHSM/f showed higher cellular retention compared to PHIM/f. The pH-induced destabilization and endosomal escape activity of PHSM/f can be credited for the remarkable difference in drug retention evident between the two micelle types. Upon the pH-triggered destabilization of micelles in the endosome, the likelihood of efflux is substantially lowered, as demonstrated by both confocal microscopy and flow cytometry. These results are consistent with studies of the endosomal disruption effects of novel liposomes carrying therapeutic anti-tumor drugs carried out by Mastrobattista et al. (37) using a similar flow cytometry technique.

Despite the fact that MDR tumor cells over-express MDR proteins (3, 9, 13, 14), it is expected that the novel PHSM/f can kinetically overcome this difficulty by triggering endosomal membrane destabilization.

FITC-labeled Polymer and DOX Elimination Kinetics

Accumulation kinetics are affected by both uptake and elimination rates. Since the uptake rates of ligand-conjugated micelles appear similar in our studies regardless of micelle type or drug resistance, we focused on the elimination kinetics of FITC-labeled polymer and DOX after incubating cells for 30 min.

Fig. 5 compares the FITC-labeled polymer fluorescence over time for PHSM/f and PHIM/f using both wild-type MCF-7 cells and MCF-7/DOX^R cells. In wild-type MCF-7 cells, PHSM/f and PHIM/f showed negligible differences in cellular polymer (FITC-labeled) concentration. However, elimination kinetics in resistant tumor cells showed dramatic differences between the two micelle types (Fig. 5). The cellular polymer concentration of PHSM/f in MCF-7/DOX^R cells was significantly higher than in PHIM/f in MCF-7/DOX^R cells after the 24-h period. The measured PHIM/f content (the FITC-labeled polymer of the micelles) in resistant tumor cells was nearly half of its initial fluorescein content by the end of the 24 h. However, the measured PHSM/f content in resistant tumor cells was approximately 90% of its initial fluorescein content after the same period of time.

As mentioned earlier, resistant cells have higher elimination rates of micelles when compared with wild-type cells and this phenomenon can be attributed to the more highly advanced efflux mechanisms of resistant cells (9–12, 38). Rapid efflux by possible folate-efflux mechanisms (22) of tumor cells was avoided in the cells treated with PHSM/f in this case because of the pH-induced destabilization of the polyHis component of the PHSM/f, which led to endosomal disruption. This mechanism was confirmed through confocal microscopy as demonstrated in Fig. 6. This figure portrays the intracellular fluorescence intensity of FITC-labeled PHSM/f or PHIM/f internalized in MCF-7/DOX^R cells after 30 min

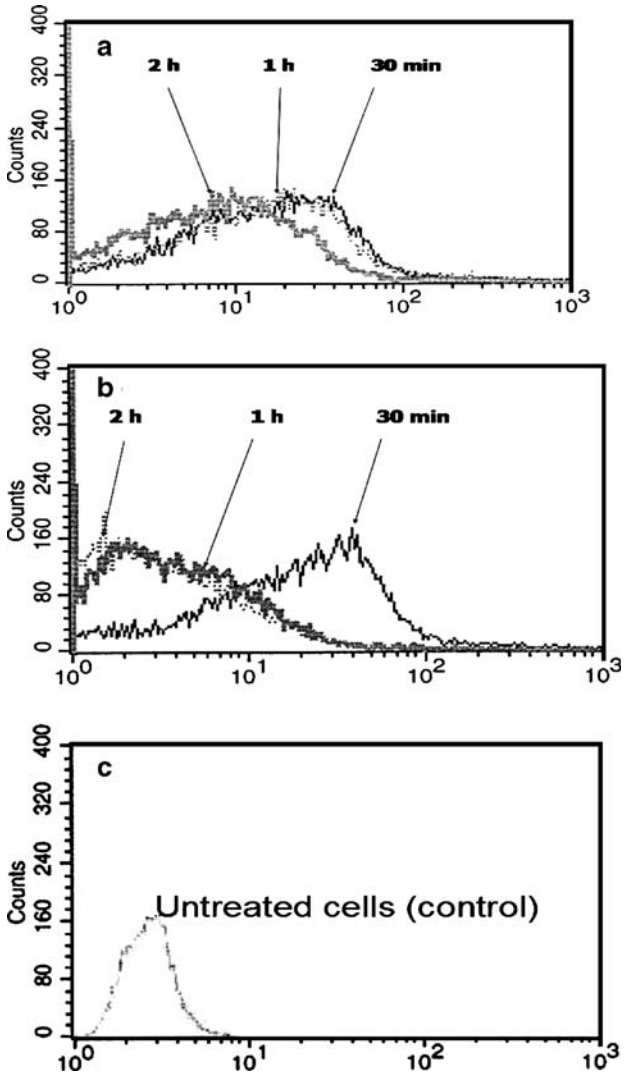

Fig. 4. Flow cytometry study revealing the fluorescence intensity of MCF-7/DOX^R cells marked with FITC-labeled polymer, at 30 min, 1 h, and 2 h, at pH 6.8 after exposing the cells to **a** PHSM/f or **b** PHIM/f for 30 min and washing. Flow cytometry result of the untreated MCF-7/DOX^R cells is shown in (**c**).

incubation, and after washing and incubating the cells for 1–2 h in fresh medium lacking micelles. The fluorescence intensity peak of PHIM/f showed more pronounced decrease than in PHSM/f as incubation time passed. This behavior is consistent with results discussed regarding Fig. 5.

Endosome recycling appears to be the major efflux mechanisms in resistant tumor cells (2–8, 13–19), thereby allowing increased exocytosis of nanoparticles entrapped in endosomes. PHIM/f are mostly sequestered in sub-organelles such as endosomes (see Fig. 3), and are then transferred out of cells by advanced exocytosis mechanisms characteristic of resistant tumor cells, where the elimination of PHIM/f in resistant cells was higher than in wild tumor cells. The kinetics of pH-induced micelle destabilization and endosomal escape activity of PHSM/f exceeded the efflux mechanisms of resistant tumor cells.

The elimination of DOX was assumed to be more complex since it was either in a free form or within the micelle core, but its collective elimination kinetics highly imitated the elimination of FITC-labeled polymers (Fig. 7). The elimination of DOX from both MCF-7/DOX^R cells and wild MCF-7 cells was measured after initial exposure with free DOX, DOX-loaded PHSM/f, or DOX-loaded PHIM/f in seven controlled experiments. The data presented in Fig. 7 is the total fluorescence intensity of DOX regardless of its cellular location (endosomes, cytosol, and nucleus) and its micelle location (inside or outside of micelles).

In Fig. 7, elimination was slower when wild-type MCF-7 cells were exposed to PHIM/f, and slowest when wild-type MCF-7 cells were exposed to PHSM/f, a pattern that was expected when comparing drug-carriers versus free DOX, and also consistent with studies in the literature (21, 39, 40). The elimination of DOX in MCF-7/DOX^R cells most accurately demonstrated the unique properties of PHSM/f, as seen in Fig. 7a. The efflux mechanisms for anti-tumor drugs in resistant tumor cells were exceeded by the kinetics of pH-induced micelle destruction and endosomal disruption activity of PHSM/f. The results clearly demonstrate that after 24 h DOX content in cells treated with PHSM/f exceeded the DOX content of cells treated with PHIM/f by a factor of 2, and exceeded the DOX content in cells treated with free DOX even more.

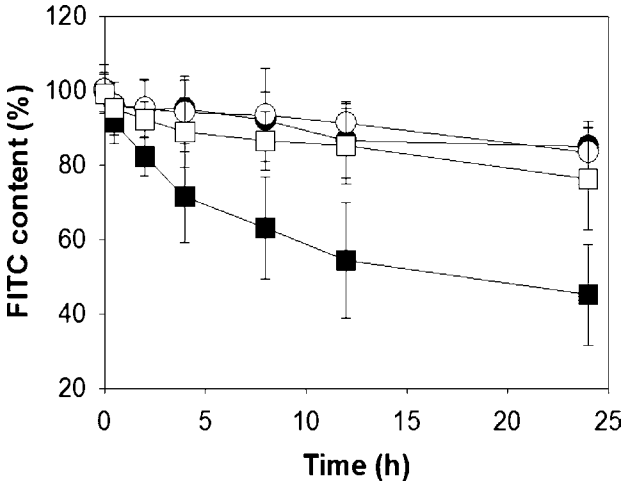

Fig. 5. The relative fluorescein content (percentage) remaining in cells in elimination trials as a function of time using FITC-labeled PHSM/f (*filled circle*) and PHIM/f (*filled square*) ($p<0.001$ compared to FITC-labeled PHSM/f) against MCF-7/DOX^R cells, and PHSM/f (*open circle*) ($p>0.1$ compared to FITC-labeled PHSM/f) or PHIM/f (*open square*) ($p>0.1$ compared to FITC-labeled PHSM/f) using wild MCF-7 cells, as a function of time ($n=7$). The fluorescein content in cells immediately following 30 min incubation was counted as 100%.

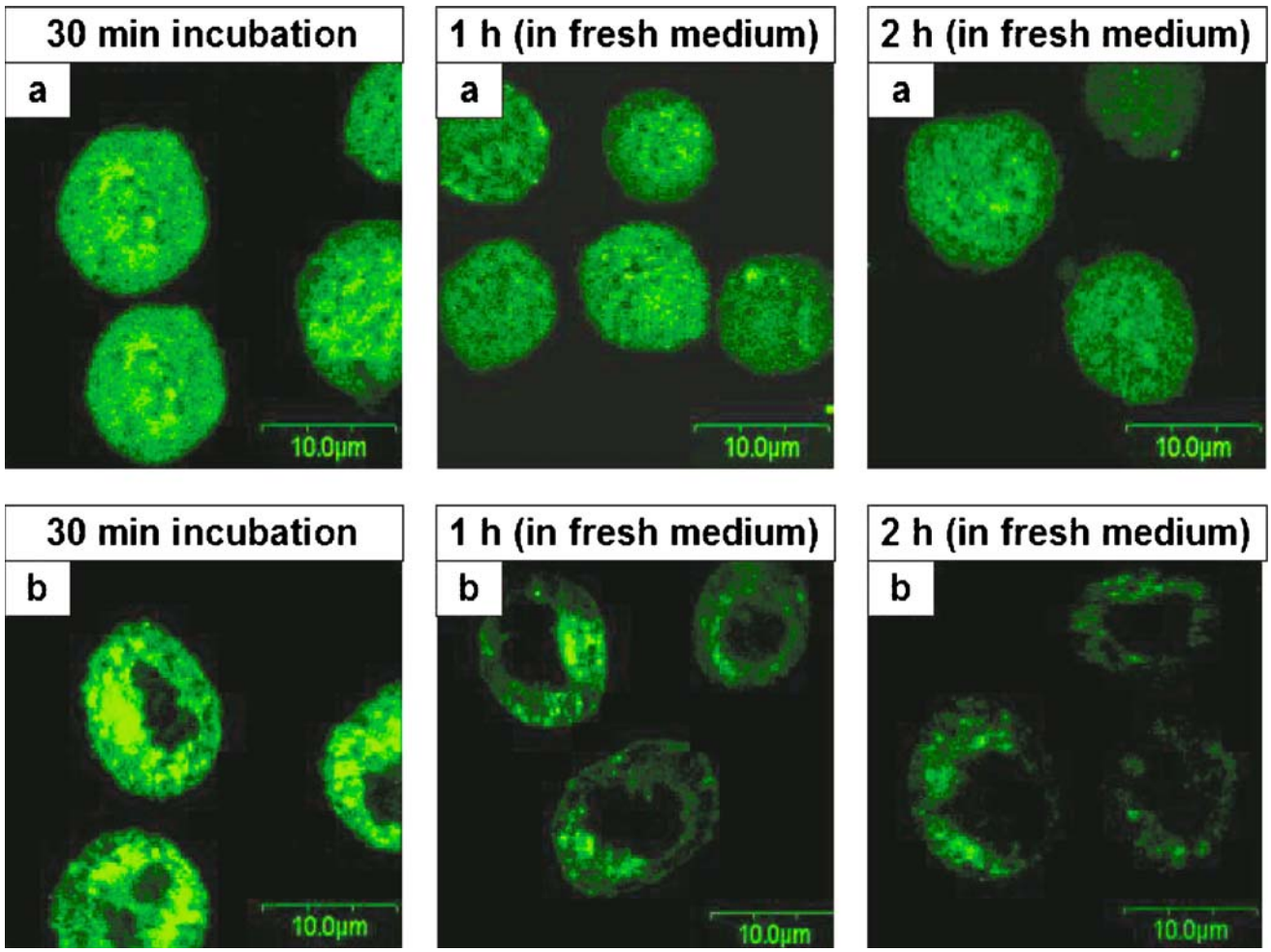

Fig. 6. Confocal microscopic pictures revealing MCF-7/DOX^R cells marked with FITC-labeled polymer after exposing the cells to **a** PHSM/f or **b** PHIM/f for 30 min and then incubation for 1 and 2 h in fresh medium without micelles.

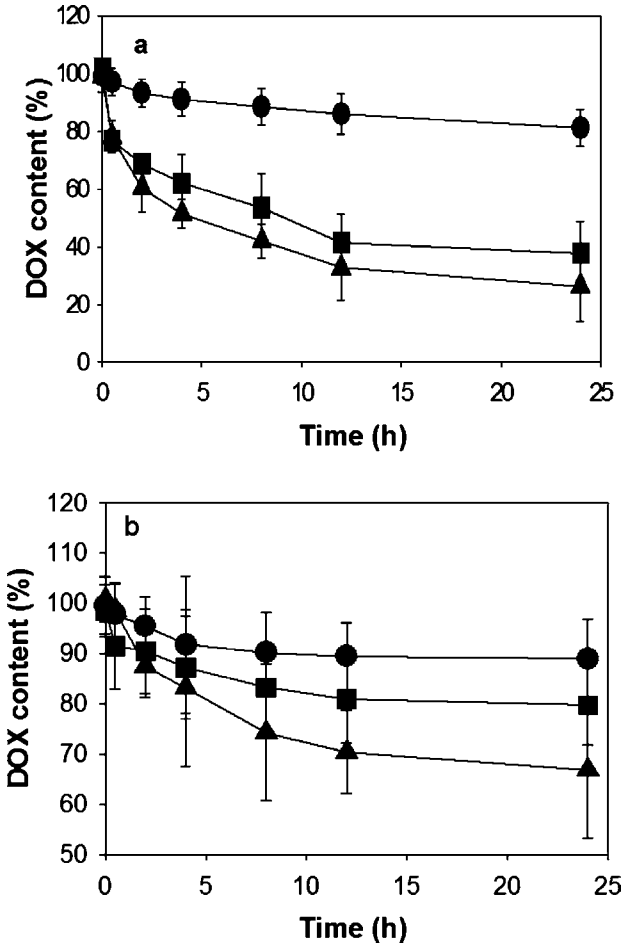

Fig. 7. The relative DOX content (percentage) remaining in cells in elimination trials using PHSM/f (*filled circle*) ($p<0.001$ compared to free DOX), PHIM/f (*filled square*) ($p<0.01$ compared to free DOX), and free DOX (*filled triangle*) against **a** MCF-7/DOX^R cells or **b** wild MCF-7 cells, as a function of time ($n=7$). The DOX content in cells right after 30 min incubation was counted as 100%.

In the case of wild MCF-7 cells, as shown in Fig. 7b, elimination followed the same pattern. Both PHSM/f and PHIM/f had an advantage over free DOX because of their folate-mediated targeting (20, 21, 26, 27, 41). Furthermore, PHSM/f had the additional advantages of pH-induced micelle destabilization and endosomal release capability over PHIM/f as described above. Consequently, PHSM/f in the endosomes abruptly released DOX within the cells and outside the endosomes, and this DOX retention was maintained over time.

DOX release rates from PHIM/f entrapped in endosomes were not significantly influenced by pH (data not shown) and the fraction of released DOX appeared to be sequestered in the endosomes. This sequestration of DOX results in its difficulty in crossing across the endosomal membrane. The elimination kinetics may be attributed to exocytosis or the recycling of endosomes containing PHIM/f and released fraction of DOX.

PHSM/f demonstrated accelerated DOX release and micelle destabilization in the endosome. This destabilization process disturbed endosomal membranes by the proton-sponge effects of polyHis and interaction with the endosomal membrane, resulting in the diffuse spread of DOX and polymers inside the cells. This process highly avoided drug elimination via endosome recycling. Of course proving this hypothesis would require further investigation through cellular pharmacokinetics studies.

CONCLUSIONS

Polymeric PHSM/f synthesized from polyHis/PEG and pLLA/PEG block copolymers with folate conjugation were investigated for their ability to enhance drug retention in MDR cells. PolyHis promoted pH-induced destabilization and endosomal drug release, reducing rapid drug efflux from MDR cells. PHSM/f exhibited accumulation patterns for FITC-labeled polymer similar to PHIM/f (lacking polyHis). However, elimination kinetics for FITC-labeled polymers and DOX varied significantly for the two-micelle types. Over a 24-h period, there was nearly 2-fold higher retention of polymer and drug using PHSM/f compared to PHIM/f counterparts. PHSM/f achieved higher drug retention at the tumor site by virtue of the possible endosomal disruption activity of the polyHis component within the micelles. Overall, this novel pH-sensitive polymeric micelle can provide not only for the targeting of tumor cells by folate-receptor recognition, but also for preserving high intracellular drug concentrations in both wild-type and resistant tumor cells.Uncited references: (4, 15, 24, 35)

ACKNOWLEDGEMENTS

The authors would like to thank Deepa Mishra (University of Utah) for carefully editing the English in this manuscript. This work was supported by NIH CA101850.

REFERENCES

1. D. Boesch, C. Gaveriaux, B. Jachez, A. Pourtier-Manzanedo, P. Bollinger, and F. Loor. In vivo circumvention of P-glycoprotein-mediated multidrug resistance of tumor cells with SDZ PSC 833. *Cancer Res.***51**:4226–4233 (1991).
2. M. Sehested, T. Skovsgarrd, B. van Deurs, and H. Winther-Nielsen. Increase in nonspecific adsorptive endocytosis in anthracycline- and vinca alkaloid-resistant Ehrlich ascites tumor cell lines. *J. Natl. Cancer Inst.***78**:171–179 (1987).
3. S. M. Simon and M. Schindler. Cell biological mechanisms of multidrug resistance in tumors. *Proc. Natl. Acad. Sci.***91**:3497–3504 (1994).
4. A. M. Cataldo, S. Petanceska, C. M. Peterhoff, N. B. Terio, C. J. Epstein, A. Villar, E. J. Carlson, M. Staufenbiel, and R. A. Nixon. App gene dosage modulates endosomal abnormalities of Alzheimer's disease in a segmental trisomy 16 mouse model of down syndrome. *J. Neurosci.* **23**:6788–6792 (2003).
5. D. A. Lazzarino, P. Blier, and I. Mellman. The monomeric guanosine triphosphatase rab4 controls an essential step on the pathway of receptor-mediated antigen processing in B cells. *J. Exp. Med.* **188**:1769–1774 (1998).
6. J. van Adelsberg and Q. Al-Awqati. Regulation of cell pH by Ca^{2+}-mediated exocytotic insertion of H-ATPase. *J. Cell Biol.***102**:1638–1645 (1998).
7. A. Hager, G. Debus, H. G. Edel, H. Stransky, and R. Serrano. Auxin induces exocytosis and the rapid synthesis of a high-turnover pool of plasma-membrane H^+ ATPase. *Planta***185**:527–537 (1991).
8. L. Warren, J. C. Jardillier, and P. Ordentlich. Secretion of lysosomal enzymes by drug-sensitive and multiple drug-resistant cells. *Cancer Res.* **51**:1996–2001 (1991).
9. J. H. Hooijberg, G. J. Peters, Y. G. Assaraf, I. Kathmann, D. G. Priest, M. A. Bunni, A. J. Veerman, G. L. Scheffer, G. J. Kaspers, and G. Jansen. The role of multidrug resistance proteins MRP1, MRP2 and MRP3 in cellular folate homeostasis. *Biochem. Pharmacol.* **65**:765–771 (2003).
10. M. M. Gottesman and I. Pastan. Biochemistry of multidrug resistance mediated by the multidrug transporter. *Annu. Rev. Biochem.* **62**:385–427 (1993).
11. S. Naito, A. Yokomizo, and H. Koga. Mechanisms of drug resistance in chemotherapy for urogenital carcinoma. *Int. J. Urol.* **6**:427–439 (1999).
12. E. Aronica, J. A. Gorter, G. H. Jansen, C. W. van Veelen, P. C. van Rijen, S. Leenstra, M. Ramkema, G. L. Scheffer, R. J. Scheper, and D. Troost. Expression and cellular distribution of multidrug transporter proteins in two major causes of medically intractable epilepsy: focal cortical dysplasia and glioneuronal tumors. *Neuroscience.***118**:417–429 (2003).
13. Y. G. Assaraf, L. Rothem, J. H. Hooijberg, M. Stark, I. Ifergan, I. Kathmann, B. A. C. Dijkmans, G. J. Peters, and G. Jansen. Loss of multidrug resistance protein 1 expression and folate efflux activity results in a highly concentrative folate transport in human leukemia cells. *J. Biol. Chem.* **278**:6680–6686 (2003).
14. Z. S. Chen, K. Lee, S. Walther, R. B. Raftogianis, M. Kuwano, H. Zeng, and G. D. Kruh. Analysis of methotrexate and folate transport by multidrug resistance protein 4 (ABCC4): MRP4 is a Component of the Methotrexate Efflux System. *Cancer Res.* **62**:3144–3150 (2002).
15. A. Reymann, A. Bunge, S. Laer, and M. Dietel. Morphological and functional features of cytostatic drug resistance and the effects of MDR modulators. *Pharmazie* **51**:171–176 (1996).
16. E. J. Demant, M. Sehested, and P. B. Jensen. A model for computer simulation of P-glycoprotein and transmembrane delta pH-mediated anthracycline transport in multidrug-resistant tumor cells. *Biochim. Biophys. Acta* **1055**:117–125 (1990).
17. J. Panyam and V. Labhasetwar. Dynmaics of endocytosis and exocytosis of poly(D,L-lactide-co-glycolide) nanoparticles in vascular smooth muscle cells. *Pharm. Res.* **20**:212–220 (2003).
18. J. S. Park, T. H. Han, K. Y. Lee, S. S. Han, J. J. Hwang, D. H. Moon, S. Y. Kim, and Y. W. Cho. N-acetyl histidine-conjugated glycol chitosan self-assembled nanoparticles for intracytoplasmic delivery of drugs: Endocytosis, exocytosis and drug release. *J. Control. Release***115**:37–45 (2006).
19. S. K. Sahoo and V. Labhasetwar. Enhanced antiproliferatively activity of transferring-conjugated paclitaxel-loaded nanoparticle is mediated via sustained intracellular drug retention. *Mol. Pharmacol.***2**:373–383 (2005).
20. J. A. Reddy and P. S. Low. Folate-mediated targeting of therapeutic and imaging agents to cancers. *Crit. Rev. Ther. Drug Carr. Syst.***15**:587–627 (1998).
21. R. J. Lee and P. S. Low. Folate-mediated tumor cell targeting of liposome-entrapped doxorubicin in vitro. *Biochem. Biophys. Acta***1233**:134–144 (1995).
22. M. Stark, L. Rothem, G. Jansen, G. L. Scheffer, I. D. Goldman, and Y. G. Assaraf. Antifolate resistance associated with loss of MRP1 expression and function in Chinese Hamster ovary cells with markedly impaired export of folate and cholate. *Mol. Pharmacol.***64**:220–227 (2003).
23. P. Midoux and M. Monsigny. Efficient gene transfer by histidylated polylysine/pDNA complexes. *Bioconjug. Chem.* **10**:406–411 (1999).
24. A. Kichler, C. Leborgne, J. Marz, O. Danos, and B. Bechinger. Histidine-rich amphipathic peptide antibiotics promote efficient delivery of DNA into mammalian cells. *Proc. Natl. Acad. Sci. U S A* **100**:1564–1568 (2003).
25. K. W. Mok and P. R. Cullis. Structural and fusogenic properties of cationic liposomes in the presence of plasmid DNA. *Biophys. J.* **73**:2534–2545 (1997).
26. E. S. Lee, K. Na, and Y. H. Bae. Doxorubicin loaded pH-sensitive polymeric micelles for reversal of resistant MCF-7 tumor. *J. Control. Release* **103**:405–418 (2005).
27. E. S. Lee, K. Na, and Y. H. Bae. Polymeric micelle for tumor pH and folate-mediated targeting. *J. Control. Release* **91**:103–113 (2003).
28. E. S. Lee, K. Na, and Y. H. Bae. Super pH-sensitive multifunctional polymeric micelle. *Nano Lett.* **5**:325–329 (2005).
29. E. S. Lee, H. J. Shin, K. Na, and Y. H. Bae. Poly(L-histidine)-PEG block copolymer micelles and pH-induced destabilization. *J. Control. Release* **90**:363–374 (2003).
30. N. Oku, N. Yamaguchi, N. Yamaguchi, S. Shibamoto, F. Ito, and M. Nango. The fusogenic effect of synthetic polycations on negatively charged lipid bilayers. *J. Biochem. (Tokyo)***100**:935–944 (1986).
31. G. M. Kim, Y. H. Bae, and W. H. Jo. pH-induced micelle formation of poly(hisitidine-co-phenylalanine)-block-poly(ethylene glycol) in aqueous media. *Macromol. Biosci.* **5**:1118–1124 (2005).
32. Z. G. Gao, D. H. Lee, D. I. Kim, and Y. H. Bae. Doxorubicin loaded pH-sensitive micelle targeting acidic extracellular pH of human ovarian A2780 tumor in mice. *J. Drug Target.* **13**:391–397 (2005).
33. L. D. Skarsgard, D. K. Acheson, A. Vinczan, B. C. Wouters, B. E. Heinrichs, D. W. Loblaw, A. I. Minchinton, and D. J. Chaplin. Cytotoxic effect of RB 6145 in human tumour cell lines: dependence on hypoxia, extra- and intracellular pH and drug accumulation. *Br. J. Cancer.***72**:1479–1486 (1995).
34. J. M. Benns, J. S. Choi, R. I. Mahato, J. S. Park, and S. W. Kim. pH-sensitive cationic polymer gene delivery vehicle: *N*-Ac-poly(L-histidine)-graft-poly(L-lysine) comb shaped polymer. *Bioconjug. Chem.***11**:637–645 (2000).
35. D. Putnam, C. A. Gentry, D. W. Pack, and R. Langer. Polymer-based gene delivery with low cytotoxicity by a unique balance of side-chain termini. *Proc. Natl. Acad. Sci.* **98**:1200–1205 (2001).
36. C. Y. Wang and L. Huang. Polyhistidine mediates an acid-dependent fusion of negatively charged liposomes. *Biochemistry* **23**:4409–4416 (1984).
37. E. Mastrobattista, D. J. Crommelin, J. Wilschut, and G. Storm. Targeted liposomes for delivery of protein-based

drugs into the cytoplasm of tumor cells. *J. Liposome Res.***12**:57–65 (2002).
38. H. Schwarzenbach. Expression of MDR1/P-glycoprotein, the multidrug resistance protein MRP, and the lung-resistance protein LRP in multiple myeloma. *Med. Oncol.***19**:87–104 (2002).
39. T. Nakanishi, S. Fukushima, K. Okamoto, M. Suzuki, Y. Matsumura, M. Yokoyama, T. Okano, Y. Sakurai, and K. Kataoka. Development of the polymer micelle carrier system for doxorubicin. *J. Control. Release* **74**:295–302 (2001).
40. K. Kataoka, T. Matsumoto, M. Yokoyama, T. Okano, Y. Sakurai, S. Fukushima, K. Okamoto, and G. S. Kwon. Doxorubicin-loaded poly(ethylene glycol)-poly(beta-benzyl-L-aspartate) copolymer micelles: their pharmaceutical characteristics and biological significance. *J. Control. Release* **64**:143–153 (2000).
41. A. Reddy and P. S. Low. Enhanced folate receptor mediated gene therapy using a novel pH-sensitive lipid formulation. *J. Control. Release* **64**:27–37 (2000).